INTRA-PATIENT REGISTRATION METHODS FOR THORACIC CT EXAMS

José Silvestre Silva
Departamento de Física, Faculdade de Ciências e Tecnologia,Universidade de Coimbra, Portugal
Centro de Instrumentação, Faculdade de Ciências e Tecnologia,Universidade de Coimbra, Portugal

João Cancela
Departamento de Física, Faculdade de Ciências e Tecnologia,Universidade de Coimbra, Portugal

Luísa Teixeira
Clínica Universitária de Imagiologia dos Hospitais da Universidade de Coimbra, Portugal

Keywords: Medical Image Analysis, Image Registration, Lung Tumours, Computed Tomography.

Abstract: Now-a-days CT scanners provide detailed morphological information of pulmonary structures, with great importance to the diagnostic and follow-up of oncological diseases. When a patient with lung cancer is submitted to several CT exams during a period of time; these exams need an appropriate registration to quantify or visualize the tumour's evolution. We propose a new method for 3D intra-patient registration of thoracic CT exams and compare its results with several 3D registration methods. The performance of these registration methods is analysed, computing several normalized figures of merit; we also explore these metrics to check which is more sensible to changes in CT exams due to the presence of lung tumours. The results with several cases of intra-patient, intra-modality registration show that the proposed method provides an accurate registration which is needed for the quantitative tracking of lesions that may effectively assist the follow-up process of oncological patients.

1 INTRODUCTION

Modern high resolution Computed Tomography scanners offer more diagnostic options and a better diagnostic quality. Consequently, it will also increase the time needed for data reading by the radiologist. Therefore, computer aid is necessary in order to increase the level of efficiency and quality in the diagnostic workflow.

Image registration geometrically aligns two images: the reference and sensed images. To register two images it is necessary to find a transformation so that each pixel in the first image can be mapped to a pixel in the second (Brown, 1992) (Blaffert & Wiemker, 2004). The image registration is used in several clinical scenarios. For instance, consider two images taken of a patient using different medical modalities or comparing two CT exams from a patient, to identify the differences between the two images in a follow-up study of an oncological patient. Although this identification can be done by the radiologist, there is always the possibility that small, but essential, features could be missed (Brown, 1992).

In the literature, it is found some work done in this area. El-Baz (El-Baz, Yuksel, Elshazly, & Farag, 2005) developed an automatic approach for the early detection of lung nodules that may lead to lung cancer. This approach involves performing rigid registration and then a non-rigid registration to compensate the lung deformation due to the heart beats and respiration of the patient; however this method cannot handle large deformations.

Matsopoulos (Matsopoulos, Mouravliansky, Asvestas, Delibasis, & Kouloulias, 2002) proposed an automatic elastic registration scheme applied on thoracic CT exams of patients diagnosed with non-small cell lung cancer.

Silvestre Silva J., Cancela J. and Teixeira L. (2009).
INTRA-PATIENT REGISTRATION METHODS FOR THORACIC CT EXAMS .
In *Proceedings of the International Conference on Bio-inspired Systems and Signal Processing*, pages 285-290
DOI: 10.5220/0001538002850290

Volumetric warping and registration of CT lung volumes have been investigated by Li (Li, Christensen, Dill, Hoffman, & Reinhardt, 2002), whose approach uses point correspondence of landmarks that are expanded over the entire volume by means of an iterative method. Although this method has shown good results for mapping lung deformation due to respiration, it requires the manual registration of landmarks.

Betke (Betke, Hong, Thomas, Prince, & Ko, 2003) developed an automated method for registering CT images of the chest; it detected anatomical landmarks: the trachea, sternum and spine, then he used an iterative lung surface registration based on minimizing Euclidean distances. The locations of the pulmonary vessel branch points and nodules were manually defined.

Blaffert (Blaffert & Wiemker, 2004) studied the precision and computation time of a rigid body using an affine and a spline based elastic registration approach on the full data volume; he compared the results to an affine registration that was preceded by a segmentation of the lung.

Boldea (Boldea, Sarrut, & Carrie, 2005) investigated the deformable registration methods for a breath-hold reproducibility study in radiotherapy, analysing internal lung residual motion between several 3D CT scans taken from the same patient, at the same level of the breathing cycle.

West (West, Maurer, & Dooley, 2005) examined the problem of deformable registration of the abdomen and was interested in modelling respiratory motion of abdominal organs, because the deformation of the lungs during the respiratory cycle can lead to the movement of others organs (liver, kidney, etc.); he used twenty-one landmarks selected manually.

Chambon (Chambon et al., 2007) presented a CT-PET landmark-based registration method that uses a breathing model to guarantee physiologically plausible deformations.

Fung (Fung, Wong, Cheng, Grimm, & Uematsu, 2005) compared two image fusion techniques for the localization of patient position during radiation release for cancer patients.

Tang (Tang, Hamarneh, & Celler, 2006) presented an automatic and accurate technique for 3D registration of SPECT and CT, which allowed the attenuation correction of SPECT images and the fusion of the anatomic details from CT and the functional information from SPECT.

Ruan (Ruan, Fessler, Robserson, Balter, & Kessler, 2007) studied a method that takes into account different types of tissues, especially bone, in non-rigid registration. Chen (Chen, Varley, Shark, Shentall, & Kirby, 2007) presented a 3D-2D image registration algorithm for pre-treatment validation in radiotherapy.

In the present work, we propose a methodology for the 3D intra-patient registration of thoracic CT exams. We compare performances analysing the processing time and the values of similarity metrics for each method. We also studied the behaviour of several normalized similarity metrics in the presence of pulmonary tumours in oncological patients.

2 METHOD

In this paper, we present a method for the registration of pulmonary CT exams and compare its performance with traditional registration method and also with two optimised registration methods. Also in this work, we search for the best metric, sensible to changes in CT exams, due to the presence of lung tumours.

2.1 Pre-processing

In the high resolution CT exams, the images are sensitive to noise, especially in the extra-thoracic region, where there is air. As noise can contribute negatively to the lung's segmentation, before any processing, and after comparing several denoising filters (J. S. Silva, Silva, & Santos, 2003), the noise is attenuated using a geometric mean filter (Sonka, Hlavac, & Boyle, 1998).

The pulmonary regions are identified using a previous developed (A. Silva, Silva, Santos, & Ferreira, 2001) (J. S. S. Silva, 2005) and validated algorithm (Santos, Ferreira, Silva, Silva, & Teixeira, 2004) producing always one contour for each lung. This algorithm uses information from the CT image histogram and, with a chain of morphological operations, identifies the left and right lung contours. Even when the lungs are visually merged, two contours are always identified, defining the frontier of left and right lungs. After pulmonary segmentation, all binary slices are joined to create one 3D pulmonary image.

Finally, in this pre-alignment step, it is computed the mass center of both 3D CT exams and performed a translation on the second exam, in order to both mass centers become coincident.

2.2 Affine Registration

The registration can be understood as the determination of spatial alignment between images. For the present method, we consider affine transformations, as the only relevant transformation (Blaffert & Wiemker, 2004).

2.2.1 Transformations

We defined the following transformation matrix: T for translation on x, y, z; R_x, R_y, R_z for rotation over 3 axis, C_{xy}, C_{xz} and C_{yz} for shearing on planes xy, xz and yz and S for scaling. The various transformation matrices are multiplied among them to obtain a global matrix, in order to process all voxels from the CT exam:

$$GLOBAL = T \times Rx \times Ry \times Rz \times Cxy \times Cxz \times Cyz \times S \quad (1)$$

In traditional 3D registration methods, all translations are iteratively searched, and for each translation all rotations are searched, and so on; processing a 3D image becomes a very long process. In order to overcome this limitation, we propose a registration method that sequentially performs each transformation.

In this proposed method, the first step is the search for the best translation, then holding this value; it searches for the best rotation over x axis. Holding these two best values; it searches for the best rotation over y axis, and so on, obtaining the best values for each transformation in a much faster approach than in traditional 3D registration methods. In the second step, it uses the best values found in the previous step as starting point, and then repeats the same procedure described in the first step, searching for new best values.

2.2.2 Boundaries

Setting boundaries for transformation is very important to reduce the processing time. For a CT exam that has been correctly acquired, it should not have a displacement of more than ¼ of width of the exam, and the patient body should not have a rotating higher that 15º on the table, otherwise the examination is considered inappropriate, because the anatomical structures may exceed the limits of the image; these are the limits used for the transformations.

To enhance the speed of our method, we start by computing the width of the CT exam and use 1/8 of the width as the step for searching the best translation, over the x, y and z axis in a range from −¼ of the exam width, to +¼ of the exam width. After searching for these axes, the best value is found comparing all values computed for the similarity metric.

The best translation is identified and using this value as the starting point, a new search is performed in a range from −1/8 of the exam width, to +1/8 of the exam width centred at the starting point, using a step of 1/16 of the exam width, which is half of the previous used step. This procedure is repeated until the step reaches the unit.

Then we search for the best rotation, following a similar procedure used for translation. Holding the translation best value found, we search for the best rotation, along the 3 rotation axis, in a range of [−15º; +15º] with a step of 7.5º. After identifying the best rotation, we use this value as the starting point and search for a new best value in a range of ± 7.5º, centred at the starting point, with a step of 7.5º/2. This procedure is repeated until the rotation step reaches the value of one degree. Similar procedures are used for scale and for shear.

2.3 Metrics

We used several normalized similarity metrics, also known as figures of merit to quantify the differences between the reference exam and the exam under analysis. These three metrics: Sum of the Absolute Differences (SAD), Correlation (R) and Normalized Mutual Information (NMI) have values between 0 (for two different images) and 1 (for two coincident images) (Fitzpatrick, Hill, & Calvin R. Maurer, 2000) (Hill, Batchelor, Holden, & Hawkes, 2001) (Pratt, 2001). The Mutual Information (MI) metric is shown to help computing the NMI.

$$SAD(A,B) = 1 - \frac{1}{N}\sum_{i}^{X}\sum_{j}^{Y}\sum_{k}^{Z}\left|A(i,j,k) - B(i-m,j-n,k-o)\right| \quad (2)$$

$$R = \frac{\sum_{i}^{X}\sum_{j}^{Y}\sum_{k}^{Z} A(i,j,k) \times B(i-m,j-n,k-o)}{\sqrt{\sum_{i}^{X}\sum_{j}^{Y}\sum_{k}^{Z} A(i,j,k)^2 \times \sum_{i}^{X}\sum_{j}^{Y}\sum_{k}^{Z} B(i-m,j-n,k-o)^2}} \quad (3)$$

$$MI(A,B) = \sum_{a\in A}\sum_{b\in B}\rho_{AB}(a,b)\log\frac{\rho_{AB}(a,b)}{\rho_A(a)\rho_B(b)} \quad (4)$$

$$NMI(A,B) = \frac{2MI(A,B)}{H(A)+H(B)} \text{ with } H(A) = -\sum_{a\in A}\rho_A(a)\log[\rho_A(a)] \quad (5)$$

where, A and B are images; N is a normalization coefficient; i, j and k are the coordinates on the image; m, n and o are the displacement values to the reference image; $\rho_{AB}(a,b)$ is the joint probability of the image and $\rho_A(a)$, $\rho_B(b)$ are the probability of images A and B, respectively.

2.4 Other Registration Methods

Two registration methods, using the Simplex algorithm and the Patter Search algorithm, were also implemented to compare their performance with the proposed method.

The Nelder-Mead Simplex algorithm is a direct search method for multidimensional unconstrained minimization. Without any derivative information, a scalar-valued nonlinear function of n real variables using only function values is minimized. The Nelder-Mead algorithm preserves at each stage a nondegenerate simplex, a volume different from zero in n dimensions which is the convex surface of $n+1$ vertices. This method starts with a simplex, specified by its $n + 1$ vertices and the related function values for each iteration. At least one test point is calculated, as well as their function values, and the iteration ends with the levels sets delimited (Lagarias, Reeds, Wright, & Wright, 1998).

The Pattern Search algorithm is also a direct search method and uses the function from a prearranged pattern of points fixed around the current best point, using shifts that guarantee determined minimal conditions in order to ensure the strong performance of the method. This process is repeated with the pattern centred on the new best point whenever certain minimal conditions are ensured. In other words, the reduction of the size of the pattern occurs and the function is sampled once again. The goal of the Pattern Search is sampled at set points which are broader than in the Simplex-based methods (Torczon, 1997) (Lewis & Torczon, 2002).

3 RESULTS AND DISCUSSION

In this section, we present the results from the comparison of our method and three other methods: the traditional registration method and two other methods with optimization algorithms: the Simplex algorithm and the Pattern Search algorithm.

In a second step we used exams from an arbitrary patient and perform the registration of all exams, to analyse the behaviour of normalized similarity metrics.

The results of all registration methods were computed on a desktop computer Intel Core 2 Quad, 4GB RAM, using Matlab.

Our dataset has 40 CT exams from 10 patients, each exam has about 100 sections, with 512×512 pixels, a resolution of 0.781×0.781×5mm^3 and each section is adjacent to its neighbours.

3.1 Comparing Registration Methods

We compare the results of several 3D registration methods, performing the intra-patient registration of two exams, acquired with one month interval.

In table 1 it is shown the results of 3D intra-patient registration of pulmonary CT exams, downsampled to 128×128×n (where n is the original number of sections), which include correlation values (initial value, after pre-processing / preliminary alignment based on mass center, final value), processing time and the number of iterations.

Table 1: Correlation values: registration of two exams from patient A.

(Patient A) Method:	Correlation values			Time (min)	No. of iterations
	Initial	Pre-align	Final		
Traditional	0.854	0.857	0.939	1830	21870
Our method	0.854	0.857	0.904	20	234
Pattern Search	0.854	0.857	0.929	116	1385
Simplex	0.854	0.857	0.878	12	128

From table 1, we see that the processing time of our method and Simplex method are much lower than the other two methods, which suggests that our method is a fast 3D registration technique, even when compared with a method that uses an optimization algorithm (Pattern Search method). We also observe that the best correlation values are obtained with the Pattern Search method (and with traditional method) and the worst value, with the Simplex Algorithm. So, the traditional method, due to the long processing time, is rejected.

In table 2 it is shown the results of 3D intra-patient registration of pulmonary CT exams, downsampled to 64×64×n (as described for table 1) and the initial / pre-processing / final values, for Normalized Mutual Information.

Table 2: Normalized Mutual Information values: registration of two exams from patient B.

(Patient B) Method:	Normalized Mutual Infor.			Time (min)	No. of iterations
	Initial	Pre-align	Final		
Traditional	0.114	0.628	0.799	1050	21870
Our method	0.114	0.628	0.705	12	234
Pattern Search	0.114	0.628	0.796	45	1579
Simplex	0.114	0.628	0.681	15	286

In table 2, we see that our method and the Simplex method accomplish the lower processing time. However, the normalized mutual information achieved by Simplex method is worse than the value obtained by our method, which suggests that our method is one of the best, in comparison with the three methods.

3.2 Metrics in Tumour Discrimination

Using six exams (A1, A2, A3, A4 A5 and A6) acquired during six months, one exam in each month, for the patient A (patient with lung cancer undergoing intensive therapy), we performed the registration using our method, of first exam A1 with second exam A2, also the first exam A1 with third exam A3, and so on, as shown in table 3. For each registration, the SAD, R and NMI metrics were computed. To reduce computational time, the exams were downsampled to $128\times128\times n$ and the lungs were segmented, producing 3D binary volumes, corresponding to the pulmonary regions.

Table 3: Intra-patient registration method, using 6 CT exams from a patient with lung cancer.

SAD	A1 w/ A2	A1 w/ A3	A1 w/ A4	A1 w/ A5	A1 w/ A6
Initial	0.937	0.891	0.924	0.817	0.900
Pre-align	0.939	0.923	0.949	0.936	0.929
Final	0.961	0.956	0.969	0.961	0.956

R	A1 w/ A2	A1 w/ A3	A1 w/ A4	A1 w/ A5	A1 w/ A6
Initial	0.854	0.742	0.831	0.598	0.766
Pre-align	0.857	0.817	0.886	0.860	0.834
Final	0.903	0.891	0.930	0.914	0.896

NMI	A1 w/ A2	A1 w/ A3	A1 w/ A4	A1 w/ A5	A1 w/ A6
Initial	0.588	0.387	0.525	0.191	0.417
Pre-align	0.594	0.512	0.640	0.584	0.537
Final	0.692	0.665	0.752	0.708	0.670

Using the data from table 3, we create a group for each metric and produce a box-plot graphic, to observe the dispersion of metric values.

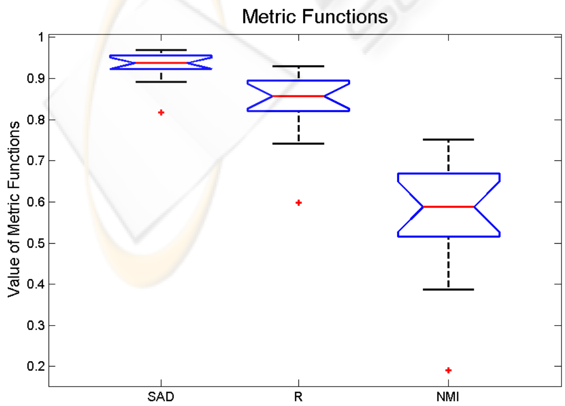

Figure 1: Dispersion values of similarity metrics.

From figure 1, and discarding the three outlier points, we see that SAD has the lower dispersion interval (values from 0.891 to 0.969) and the NMI has the higher dispersion interval (values from 0.387 to 0.752) which suggests that NMI is more sensible to the presence of tumours.

These results were confirmed with results from intra-patient registration of CT exams, using other patients with lung cancer.

4 CONCLUSIONS

In this paper, we addressed the problem of registering volumetric pulmonary CT exams of patients with lung cancer. We propose an automatic 3D intra-patient registration method. It starts by segmenting the lungs and building a 3D binary image of the pulmonary region. The centre of mass is computed and the exams are coarsely aligned. Then, a 3D registration is performed using a downsampled volume from the original 3D image. The performance of our method is compared with the traditional registration method and also with two optimised methods and we conclude that our method is the best compromise between processing time and similarity metric values.

Also, we compare the results of several normalized similarity metrics used in the 3D registration of CT exams and conclude that normalized mutual information is the metric more sensible to the changes in CT exams due to the presence of lung tumours.

The results with several cases of intra-patient, intra-modality registration show that this method provides accurate registration which is needed for the quantitative tracking of lesions that may effectively assist the follow-up process of oncological patients.

REFERENCES

Betke, M., Hong, H., Thomas, D., Prince, C., & Ko, J. P. (2003). Landmark Detection in the Chest and Registration of Lung Surfaces with an Application to Nodule Registration. *Medical Image Analysis, 7*(3), 265-281.

Blaffert, T., & Wiemker, R. (2004). Comparison of different follow-up lung registration methods with and without segmentation. *SPIE Medical Imaging 2004, 5370*, 1701-1708.

Boldea, V., Sarrut, D., & Carrie, C. (2005). Comparison of 3D Dense Deformable Registration Methods for Breath-hold Reproducibility Study in Radiotherapy.

SPIE Medical Imaging: Visualization, Image-Guided Procedures, and Display, 5747, 222-230.

Brown, L. G. (1992). A Survey of Image Registration Techniques. *ACM Computing Surveys, 24*(4), 325-376.

Chambon, S., Moreno, A., Santhanam, A. P., Rolland, J. P., Angelini, E., & Bloch, I. (2007). CT-PET Landmark-based Lung Registration Using a Dynamic Breathing Model. *Proceedings of the 14th International Conference on Image Analysis and Processing (ICIAP 2007) - Volume 00*, 691-696.

Chen, X., Varley, M. R., Shark, L.-K., Shentall, G. S., & Kirby, M. C. (2007). Automatic 3D-2D image registration using partial digitally reconstructed radiographs along projected anatomic contours. *Proc. of International Conference on Medical Information Visualisation - BioMedical Visualisation (MediViz 2007)*, 3-8.

El-Baz, A., Yuksel, S., Elshazly, S., & Farag, A. (2005). Non-rigid registration techniques for automatic follow-up of lung nodules. *Proc. of Computer Assisted Radiology and Surgery (CARS'05), Berlin, Germany*, 1115-1120.

Fitzpatrick, J. M., Hill, D. L. G., & Calvin R. Maurer, J. (2000). Image Registration. In M. Sonka & J. M. Fitzpatrick (Eds.), *Handbook of Medical Imaging* (Vol. 2, pp. 447 - 514): SPIE Press.

Fung, A. Y. C., Wong, J. R., Cheng, C.-W., Grimm, S. L., & Uematsu, M. (2005). A comparison of two image fusion techniques in CT-on-Rails localization of radiation delivery. *Physica Medica, 21*(3), 113-119.

Hill, D. L. G., Batchelor, P. G., Holden, M., & Hawkes, D. J. (2001). Medical image registration. *Physics in Medicine and Biology, 46*(3), 1- 45.

Lagarias, J. C., Reeds, J. A., Wright, M. H., & Wright, P. E. (1998). Convergence Properties of the Nelder-Mead Simplex Method in Low Dimensions. *SIAM J. on Optimization, 9*(1), 112-147.

Lewis, R. M., & Torczon, V. (2002). A Globally Convergent Augmented Lagrangian Pattern Search Algorithm for Optimization with General Constraints and Simple Bounds. *SIAM J. on Optimization, 12*(4), 1075-1089.

Li, B., Christensen, G. E., Dill, J., Hoffman, E. A., & Reinhardt, J. M. (2002). 3D inter-subject warping and registration of pulmonary CT images for a human lung model. *SPIE - Medical Imaging 2002: Physiology and Function from Multidimensional Images, 4683*, 324-335.

Matsopoulos, G. K., Mouravliansky, N. A., Asvestas, P. A., Delibasis, K. K., & Kouloulias, V. (2002). Thoracic non-rigid registration combining self-organizing maps and radial basis functions. *Med Phys., 29*(2), 201-213.

Pratt, W. K. (2001). *Digital Image Processing*: John Wiley & Sons, Inc.

Ruan, D., Fessler, J. A., Robserson, M., Balter, J., & Kessler, M. (2007). Nonrigid Registration with Regularization Incorporating Local Tissue Rigidity. *Phys. Med. Biol. (in revision).*

Santos, B. S., Ferreira, C., Silva, J. S., Silva, A., & Teixeira, L. (2004). Quantitative Evaluation of a Pulmonary Contour Segmentation Algorithm in X-ray Computed Tomography Images. *Academic Radiology, 11*(8), 868-878.

Silva, A., Silva, J. S., Santos, B. S., & Ferreira, C. (2001). Fast Pulmonary Contour Extraction in X-ray CT Images: A Methodology and Quality Assessment. *SPIE - Medical Imaging 2001: Physiology and Function from Multidimensional Images, 4321*, 216-224.

Silva, J. S., Silva, A., & Santos, B. S. (2003). Denoising Methods in High-Resolution X-Ray Computed Tomography. *Proceedings of BioEng 2003 - 7th Portuguese Conference on Biomedical Engineering*, 59 (extended version in CD of Proceedings).

Silva, J. S. S. (2005). *Segmentação Pulmonar em Estudos de Tomografia Axial Computorizada*: PhD Thesis (in Portuguese), Universidade de Aveiro.

Sonka, M., Hlavac, V., & Boyle, R. (1998). *Image Processing, Analysis, and Machine Vision* (2nd ed.): PWS Publishing.

Tang, L., Hamarneh, G., & Celler, A. (2006). Co-registration of Bone CT and SPECT Images Using Mutual Information. *IEEE Symposium on Signal Processing and Information Technology*, 116-121.

Torczon, V. (1997). On the Convergence of Pattern Search Algorithms. *SIAM J. on Optimization, 7*(1), 1-25.

West, J. B., Maurer, C. R., & Dooley, J. R. (2005). Hybrid point-and-intensity-based deformable registration for abdominal CT images. *Proceedings of SPIE Medical Imaging 2005, 5747*, 204-211.